Supporting Online Materials for:

Inner Core Differential Motion Confirmed by Earthquake Waveform

Doublets

by Jian Zhang, Xiaodong Song, Yingchun Li, Paul G. Richards,

Xinlei Sun, Felix Waldhauser

Materials and Methods

Data sources

Our data are vertical-component short-period records, processed to have the same instrument response at each station. A band-pass filter with corner frequencies ranging from 0.4 to 3 Hz is applied to both members of a doublet to enhance the signal to noise ratio (Table S2). Signals after 1981 are derived from digital seismographic stations of the International Monitoring System (IMS), the U.S. Atomic Energy Detection System (USAEDS), the Global Seismographic Network (GSN), and the Alaska Seismic Network (ASN). The data for events prior to 1981 are digitized from short-period analog World-Wide Standardized Seismograph Network records (Song, 2000a). The computer software we used to digitize the seismograms (nXscan, developed initially at California Institute of Technology) is an interactive and semi-automatic program, which can trace automatically small amplitude segments. The capability makes it possible to match not only the main phases, but also the coda waveforms wiggle by wiggle in a perfect doublet when one or two of the traces are digitized from analog records.

Double-difference analysis

We performed a double-difference (DD) analysis (Waldhauser and Ellsworth, 2000) of phase pick and cross correlation data for the doublet 93&03 to constrain their relative location. We determined cross-correlation differential arrival times at 10 stations with a range of distances and azimuths (see Fig. S7A). A 20 s window was used, starting 5 s before the manually picked onset of each phase. Three measurements were made on the first arriving P phase, five on $PKP(BC)$, one on $PKP(DF)$, and one on $PKP(AB)$. Cross-correlation coefficients are between 0.84 and 0.97. In the DD analysis we inverted the cross-correlation data together with 30 differential travel times determined from carefully examined phase picks listed in the Earthquake Data Report (EDR) bulletin. RMS residuals of the final locations are 16 msec for the cross-correlation data and 26 msec for the phase pick data. This compares to an RMS residual of 70 msec before relocation. Map view and cross-sections of the relocated doublet are shown in Fig. S7, B, C, and D. The results show that the two events are separated by less than 1 km horizontally, and about 100 m vertically. Because the rupture area for events of this magnitude is about 20 km^2 for a 3 MPa stress drop source, we conclude that the rupture areas of these two events substantially overlap.

Investigating the effect of source separation

In order to investigate the effect that a few km source separation would have on the observed $dt(BC - DF)$ for the two events at a fixed station, we used waveforms for the earlier event of the doublet 93&03 recorded at 20 channels within the Eielson array of the

International Monitoring System (IMS) to measure the change of the differential travel times between BC and DF with respect to change of epicentral distance. The measured rate of 0.013 s/km (Fig. S8) is far too small a value to allow plausible mislocation of less than 1 km (Fig. S7) to cause the observed temporal changes in $d(BC - DF)$, which amount to about 0.1 s for each channel of Eielson array. In this array analysis, waveform cross-correlation is used to obtain 190 measurements. For observed $d(BC - DF)$ at 58 stations used in Fig. 3, measurements are obtained by visually picking the first prominent peaks or troughs of the coherent DF and BC phases. The difference in measured values of these two techniques was found at 20 channels of the Eielson array to be less than 0.02 s.

Correction for source separation using $d(AB - BC)$ measurements

Even for the best doublets such as in this study, the $d(AB - BC)$ is not exactly zero (Table S2). The small value (average of 0.019±0.041 s) is caused by a slight difference in event location, small-scale heterogeneity of Earth structure, and random noise. In addition, the station at College, Alaska moved to another site in 1996 (the station code was changed from COL to COLA). The two sites are separated by 4.0 km and COLA is further away from the SSI region by 2.1 km in epicentral distance, which is expected to cause 0.016 s increase (using a standard Earth model) in $BC - DF$ times. This change of station site affects four doublets with one event recorded at COL and the other at COLA. The data in Fig. 4 have been corrected for this site change.

To improve further the accuracy of $d(BC - DF)$ measurements, we can correct partly

for the influences of the factors (such as small source separations) that affect $d(BC-DF)$ and $d(AB-BC)$ values simultaneously, by constructing an empirical calibration curve of $d(BC-DF)$ and $d(AB-BC)$ values using earthquake pairs at somewhat different locations with small time separation that have similar DF, BC, and AB waveforms (Fig. S9). When the time separation is small, the effect of inner core rotation on $d(BC-DF)$ is expected to be minimum. We obtain a calibration ratio of 0.434±0.067, i.e., 0.1 s difference in $d(AB-BC)$ times corresponds to 0.043 s difference in $d(BC-DF)$ times, which is similar to predicted ratios of 0.44 and 0.38 from standard Earth models of AK135 (Kennett et al., 1995) and PREM (Dziewonski and Anderson, 1981), respectively.

Our best recorded doublet 93&03 provides a remarkable test for using $d(AB-BC)$ value to predict the relative distance of the two events to Alaska. The DD relocation indicates that the two events of this doublet are separated by 0.8 km and Event 03 is 0.8 km closer to Alaska than Event 93. The $d(AB-BC)$ value (0.02 s) for this doublet recorded at station COL and COLA indicates that Event 03 is 1.0 km closer to Alaska (using the AK135 model), in very good agreement with the DD locations. Although we have only one example here, the agreement between relative locations from DD and $d(AB-BC)$ measurement provides an indication of the level of precision (about 0.01 s in relative time and a fraction of 1 km in relative location) achievable for such high quality waveform doublets.

Our estimate of the temporal change of $BC-DF$ times using the corrected data is 0.0090±0.0005 s/year (Table S4). This value is only slightly smaller than the estimate

using the data without the correction (Fig. 4), 0.0092±0.0004 s/year. The difference has little statistical significance (they are well within one standard error of each other).

References for Supporting Online Materials

Dziewonski, A.M., and D.L. Anderson, Preliminary reference Earth model, *Phys. Earth Planet. Inter.*, *25*, 297-356, 1981.

Kennett, B.L.N., E.R. Engdahl, and R. Buland, Constraints on seismic velocities in the Earth from travel-times, *Geophys. J. Int.*, *122*, 108-124, 1995.

Li, A.Y., and P.G. Richards, Using earthquake doublets to study inner core rotation and seismicity catalog precision, *Geochem. Geophys. Geosys.*, 4(9), 1072, doi:10.1029/2002GC000379, 2003.

Song, X.D., Joint inversion for inner core rotation, inner core anisotropy, and mantle heterogeneity, *J. Geophys. Res.*, *105*, 7931-7943, 2000a.

Song, X.D., Time dependence of PKP(BC)-PKP(DF) times: Could it be an artifact of potential systematic earthquake mislocations? *Phys. Earth. Planet. Inter.*, *122*, 221-228, 2000b.

Waldhauser, F., and W.L. Ellsworth, A double-difference earthquake location algorithm: Method and application to the Northern Hayward Fault, California, *Bull. Seismol. Soc. Am.*, *90(6)*, 1353-1368, 2000.

Table S1. List of Doublet Earthquakes in South Sandwich Islands (PDE location)

Event ID	Date, Year m d	Time, h m s	Latitude, deg	Longitude, deg	Depth, km	m_b
61	1961 08 01	09 24 22.4	-56.800	-24.000	61	N/A
62	1962 06 29	03 30 18.8	-56.200	-26.900	25	N/A
64	1964 06 11	10 55 06.2	-56.000	-27.300	33	N/A
70	1970 05 25	22 45 35.2	-57.419	-25.773	61	5.6
82a	1982 03 22	18 46 05.2	-56.017	-27.226	139	5.1
82b	1982 04 30	07 46 47.8	-56.245	-27.457	106	5.7
84	1984 10 21	09 12 59.8	-56.864	-24.973	33	5.1
86a	1986 03 15	18 32 10.7	-55.931	-27.429	90	5.9
86b	1986 07 09	13 58 57.8	-56.010	-27.525	134	5.1
86c	1986 11 18	12 02 27.8	-57.933	-25.392	67	5.6
86d	1986 11 22	06 14 03.3	-56.140	-27.142	151	5.1
87a	1987 03 03	14 20 32.3	-57.910	-25.147	25	5.4
87b	1987 03 28	05 04 10.8	-57.919	-25.386	33	5.5
87c	1987 11 05	03 19 52.0	-56.018	-27.468	135	5.1
90	1990 12 08	06 03 13.4	-57.877	-25.152	33	5.4
93a	1993 09 09	21 52 12.8	-56.214	-27.332	110	5.8
93b	1993 12 01	00 59 01.2	-57.475	-25.685	33	5.5
93c	1993 12 30	17 45 00.3	-58.956	-25.356	10	5.0
95a	1995 01 03	02 54 56.9	-56.206	-27.285	130	5.5
95b	1995 08 14	08 21 43.9	-57.874	-25.397	33	5.2
95c	1995 10 24	09 25 33.0	-56.297	-26.558	33	4.7
97a	1997 04 04	02 35 44.8	-57.893	-25.599	33	4.8
97b	1997 06 02	04 57 07.6	-56.321	-27.385	99	4.9
98	1998 12 26	12 14 37.4	-56.483	-27.366	110	5.4
99	1999 05 14	05 05 08.2	-57.943	-25.452	33	4.7
01	2001 01 29	09 14 29.8	-58.909	-25.473	33	4.8
02a	2002 05 08	14 59 53.6	-56.129	-26.625	33	4.8
02b	2002 11 12	01 46 48.9	-56.550	-27.536	120	6.0
03	2003 09 06	15 46 59.9	-57.419	-25.639	33	5.6
04	2004 05 07	09 50 31.6	-57.907	-25.535	71	5.1

Table S2. Measurements of South Sandwich Islands Doublets[a]

Doublet ID	Time Lapse, yr	d(BC-DF), s	d(AB-BC), s	C.C. Coeff.	Filter, Hz	Loc. Diff., km	No. Sta.
d-2-97a-99-BC04	2.08	0.01	0.00	0.99	0.6-2.0	10.4	39[b]
d-3-87a-90	3.77	0.03	-0.01	0.96	0.6-1.5	3.7	2
d-4-98-02b	3.88	0.00	-0.02	0.95	0.8-1.5	12.9	5
d-7-95c-02a-BC01	6.50	0.06	0.00	0.99	1.0-2.0	19.2	38[b]
d-7-86d-93	6.80	0.08	0.00	0.86	0.8-2.0	14.5	1
d-7-93c-01-BC01	7.08	0.09	0.01	0.94	1.0-2.0	8.5	31[b]
d-8-87b-95[1]	8.38	0.14	-0.01	0.99	0.8-1.5	5.1	4
d-13-82b-95a	12.68	0.07	0.01	0.91	0.6-3.0	11.6	2
d-18-86c-04	17.47	0.17	0.06	0.86	0.8-2.0	9.0	3
d-18-64-82a	17.77	0.20	-0.02	0.92	0.5-2.0	5.0	1
d-23-61-84	23.22	0.17	-0.03	0.88	0.4-2.0	59.9	1
d-35-62-97b	34.93	0.34	0.07	0.79	0.6-2.0	33.0	1
t1-0-86a-86b	0.32	0.00	0.09	0.91	0.6-2.0	10.7	2
t1-1-86b-87c	1.33	0.02	-0.04	0.90	0.6-2.0	3.7	2
t1-1-86a-87c	1.64	0.02	0.05	0.94	0.6-2.0	10.0	1
t2-10-93b-03	9.76	0.11	0.02	0.91	0.6-2.0	6.8	102
t2-23-70-93b	23.52	0.24	0.05	0.90	0.6-2.0	8.2	3
t2-33-70-03	33.28	0.34	0.06	0.84	0.6-2.0	8.1	2

[a]The doublet identification (ID) indicates whether it is a doublet or a triplet and the years and the year difference of the two events. All the doublets were recorded at College, Alaska station except three doublets that were recorded at Beaver Creek array stations as noted. [1]The cited doublet [1] was first discovered by Li and Richards (2003). The cross-correlation coefficients (C.C. Coef.) are measured using BC and AB time windows (about 12 s). The location difference (Loc. Diff.) is the horizontal separation calculated using the PDE catalog. The parameter (No. Sta.) indicates the number of stations that we have data for both events. [b]These doublets were recorded by at Beaver Creek array with clear DF signals. They were also recorded by other IMS and USAEDS array stations and global network stations but without clear DF signals.

Table S3. Station information and measurements of *d(BC-DF)* for the doublet 93&03. The epicentral distance and azimuth are calculated using the U. S. Geological Survey's Earthquake Data Report location of the event 2003/09/06.

Station Code	Latitude deg	Longitude deg	Distance deg	Azimuth deg	*d(BC-DF)* sec	Filter Hz
		IMS stations in Alaska				
Eielson array ILAR (20 channels)						
IL01	64.771599	-146.886093	151.7	309.5	0.10	0.8-2.0
IL02	64.784698	-146.864303	151.7	309.5	0.09	0.8-2.0
IL03	64.771400	-146.851196	151.6	309.5	0.10	0.8-2.0
IL04	64.757004	-146.876098	151.6	309.5	0.10	0.8-2.0
IL05	64.773102	-146.922897	151.7	309.5	0.09	0.8-2.0
IL06	64.779198	-146.904006	151.7	309.5	0.08	0.8-2.0
IL07	64.799301	-146.839294	151.6	309.6	0.10	0.8-2.0
IL08	64.790298	-146.796905	151.6	309.5	0.09	0.8-2.0
IL09	64.768097	-146.783203	151.6	309.5	0.10	0.8-2.0
IL10	64.752899	-146.843093	151.6	309.5	0.08	0.8-2.0
IL11	64.741501	-146.897399	151.7	309.4	0.10	0.8-2.0
IL12	64.744698	-146.943603	151.7	309.4	0.11	0.8-2.0
IL13	64.747902	-146.986495	151.7	309.4	0.09	0.8-2.0
IL14	64.775002	-146.979400	151.7	309.5	0.08	0.8-2.0
IL15	64.777702	-146.942794	151.7	309.5	0.08	0.8-2.0
IL16	64.793297	-146.921493	151.7	309.5	0.08	0.8-2.0
IL17	64.807198	-146.889801	151.7	309.6	0.09	0.8-2.0
IL18	64.757500	-146.776794	151.6	309.5	0.09	0.8-2.0
IL19	64.746101	-146.797393	151.6	309.5	0.08	0.8-2.0
IL31	64.771400	-146.886596	151.7	309.5	0.10	0.8-2.0
		USAEDS stations				
Beaver Creek array BCAR (5 channels)						
BC01	63.0619	-141.8279	149.0	307.4	0.10	0.5-1.0
BC02	63.0440	-141.8021	149.0	307.4	0.09	0.5-1.0
BC03	63.0656	-141.7851	149.0	307.4	0.09	0.5-1.0
BC04	63.0809	-141.7684	149.0	307.5	0.09	0.5-1.0
BC05	63.0610	-141.7534	149.0	307.4	0.10	0.5-1.0

Table S3. (continued)

Burnt Mountain array BMAR (5 channels)

BM01	67.4507	-144.5273	151.3	315.4	0.16	0.8-2.0
BM02	67.4297	-144.4915	151.2	315.4	0.19	0.8-2.0
BM03	67.4192	-144.6071	151.3	315.3	0.18	0.8-2.0
BM04	67.4181	-144.5584	151.3	315.3	0.17	0.8-2.0
BM05	67.4289	-144.5807	151.4	315.3	0.18	0.8-2.0

Indian Mountain array IMAR (5 channels)

IM01	65.9969	-153.7225	154.7	311.2	0.11	0.8-2.0
IM02	66.0005	-153.7971	154.7	311.2	0.09	0.8-2.0
IM03	65.9835	-153.7491	154.7	311.1	0.10	0.8-2.0
IM04	65.9745	-153.7828	154.7	311.1	0.14	0.8-2.0
IM05	65.9751	-153.7253	154.7	311.1	0.12	0.8-2.0
TT01	62.9066	-156.0204	155.3	303.6	0.06	0.8-2.0

ASN stations

BAL	61.0353	-142.3471	148.5	303.6	0.13	0.8-2.0
BGL	61.2670	-152.3882	153.2	300.8	0.09	0.8-2.0
CCB	64.6467	-147.8054	152.0	309.0	0.18	0.5-1.0
CKT	61.2008	-152.2061	153.1	300.7	0.06	0.5-1.0
CTG	60.9660	-141.3382	148.1	303.8	0.13	0.8-2.0
CUT	62.4047	-150.2694	152.6	303.8	0.18	0.5-1.0
DOT	63.6487	-144.0624	150.2	307.9	0.10	0.5-1.0
FYU	66.5660	-145.2316	151.4	313.5	0.17	0.5-1.0
GLM	64.9873	-147.3889	151.9	309.8	0.15	0.5-1.0
HDA	64.4057	-146.9407	151.6	308.7	0.15	0.5-1.0
IMA	66.0685	-153.6786	154.7	311.3	0.10	0.8-2.0
MCK	63.7323	-148.9349	152.3	306.9	0.13	0.5-1.0
MDM	64.9588	-148.2291	152.3	309.6	0.10	0.8-2.0
NCT	60.5631	-152.9260	153.3	299.1	0.03	0.5-1.0
PLR	61.5922	-149.1307	151.8	302.4	0.07	0.8-2.0
TOA	62.1048	-146.1722	150.6	304.3	0.12	0.8-2.0
TRF	63.4510	-150.2872	152.8	306.0	0.21	0.5-1.0
TTA	62.9300	-156.0219	155.3	303.6	0.10	0.8-2.0
WRH	64.4713	-148.0897	152.1	308.6	0.15	0.5-1.0

IMS stations in Canada

INK	68.3067	-133.5200	147.4	318.9	0.11	0.8-2.0
DAWY	64.0655	-139.3909	148.3	309.9	0.10	0.8-2.0

Table S4. Estimates of Temporal Change of BC-DF Time[a]

Model	1	2	3	4
	bT	a+bT	ave. b_i (T >17 yrs)	bT (t2)
No. Pairs	15	15	6	3
a (σ_a), s	N/A	-0.002 (0.013)	N/A	N/A
b (σ_b), s/yr	0.00899 (0.00048)	0.00908 (-0.00078)	0.00907 (0.00158)	0.00907 (0.00016)
Var. Red.	91%	91%	82%	99%

[a]The estimates of temporal change is obtained by linear fitting of d(BC-DF) values with time separation (T). The d(BC-DF) values used here have been corrected for small values of d(AB-BC) (see supporting online text). Model 2, which includes the intercept term a as a free parameter, yields an intercept of essentially zero and a slope essentially the same as Model 1, which does not include an intercept. This is consistent with the notion that no temporal change is expected when there is no time lapse. Estimates using only a few pairs with large time lapses (Model 3 and Model 4) are remarkably consistent with Model 1 or Model 2.

Table S5. Estimates of Inner Core Rotation Rates

Lateral gradient from Song (2000a) (with and without mantle correction), %/°	BC-DF temporal change
	0.0090 s/year
	Eastwards Rotation Rate, °/year
-0.0145 (station and source)	0.53
-0.0176 (station only)	0.43
-0.0278 (no mantle correction)	0.27
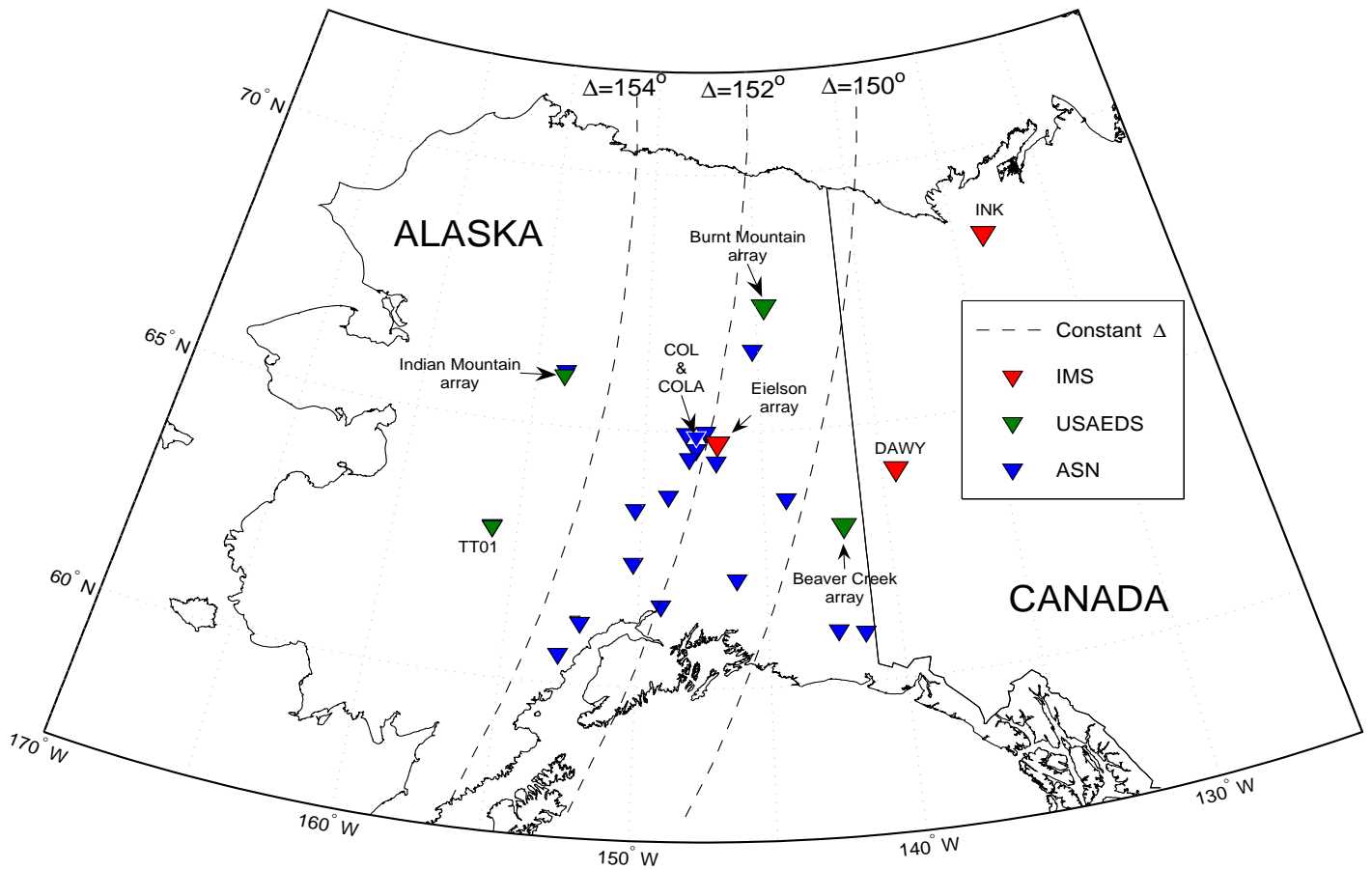
Fig. S1. Map of stations in Alaska and Canada which detected the South Sandwich Islands earthquake doublets reported in this study. These stations (a total of 58, including array stations) showed compelling evidence for temporal change of travel times through the inner core. Three dashed lines show points with constant epicentral distances from the best-recorded doublet 93&03.
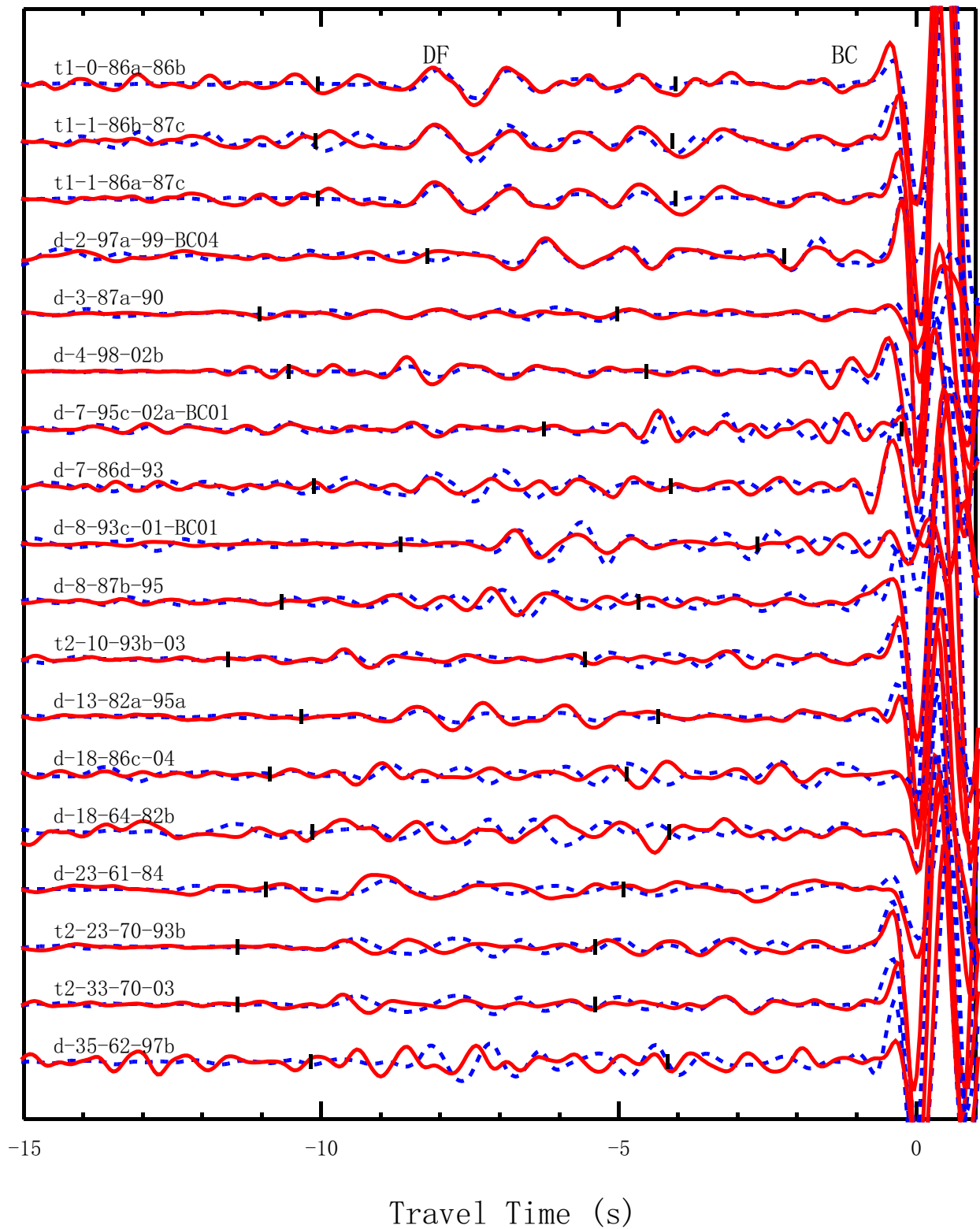
Fig. S2. Enlarged view of DF segments and the beginning part of the BC phase of the SSI doublets at Beaver Creek array and COL stations. The traces are aligned with the BC phase. The early and later events of each doublet are indicated by the blue dashed and red solid traces, respectively. The time window is expanded to show the noise levels before the DF arrivals. The DF segments indicated by the tick marks are shown in Fig. 2B.
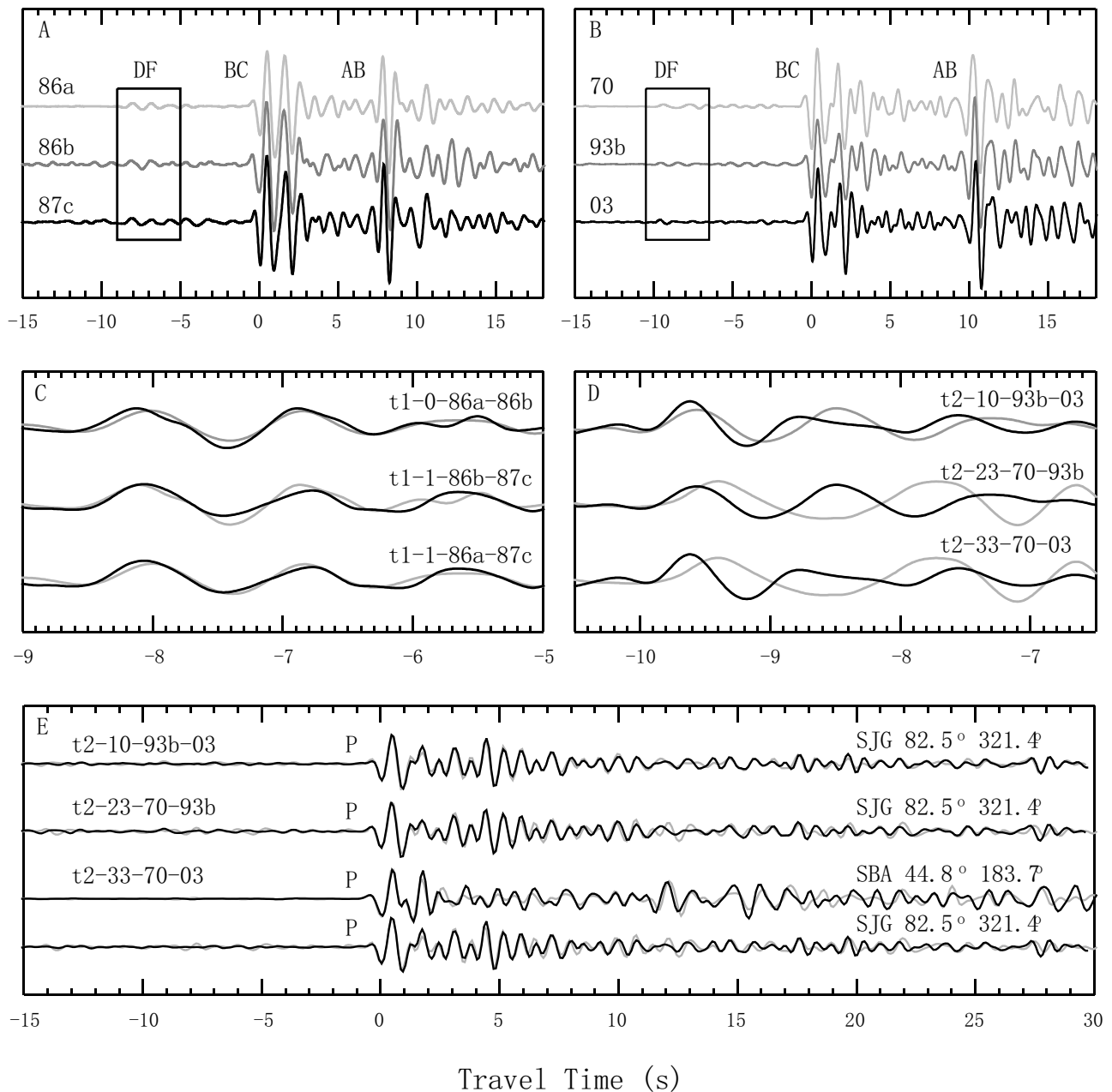
Fig. S3. Overlays of waveforms of two earthquake triplets in SSI. (**A**) Triplet t1 recorded at COL with short time separations between the events. (**B**) Triplet t2 recorded at COL with long time separations between the events. (**C, D**) Enlarged view of the DF phase (indicated in the box) for triplets t1 and t2, respectively. (**E**) P waves of triplet t2 recorded at San Juan, Puerto Rico (SJG) and Scott Base, Antarctica (SBA) at distances of 82.5° and 44.8°, respectively, and azimuths of 321.4° and 183.7°, respectively. Note the waveforms for the event in 1970 are digitized from analog records. Despite the lower resolution from the digitization than that of the digital records of other events, the P waveforms of the triplet still show remarkable similarity.
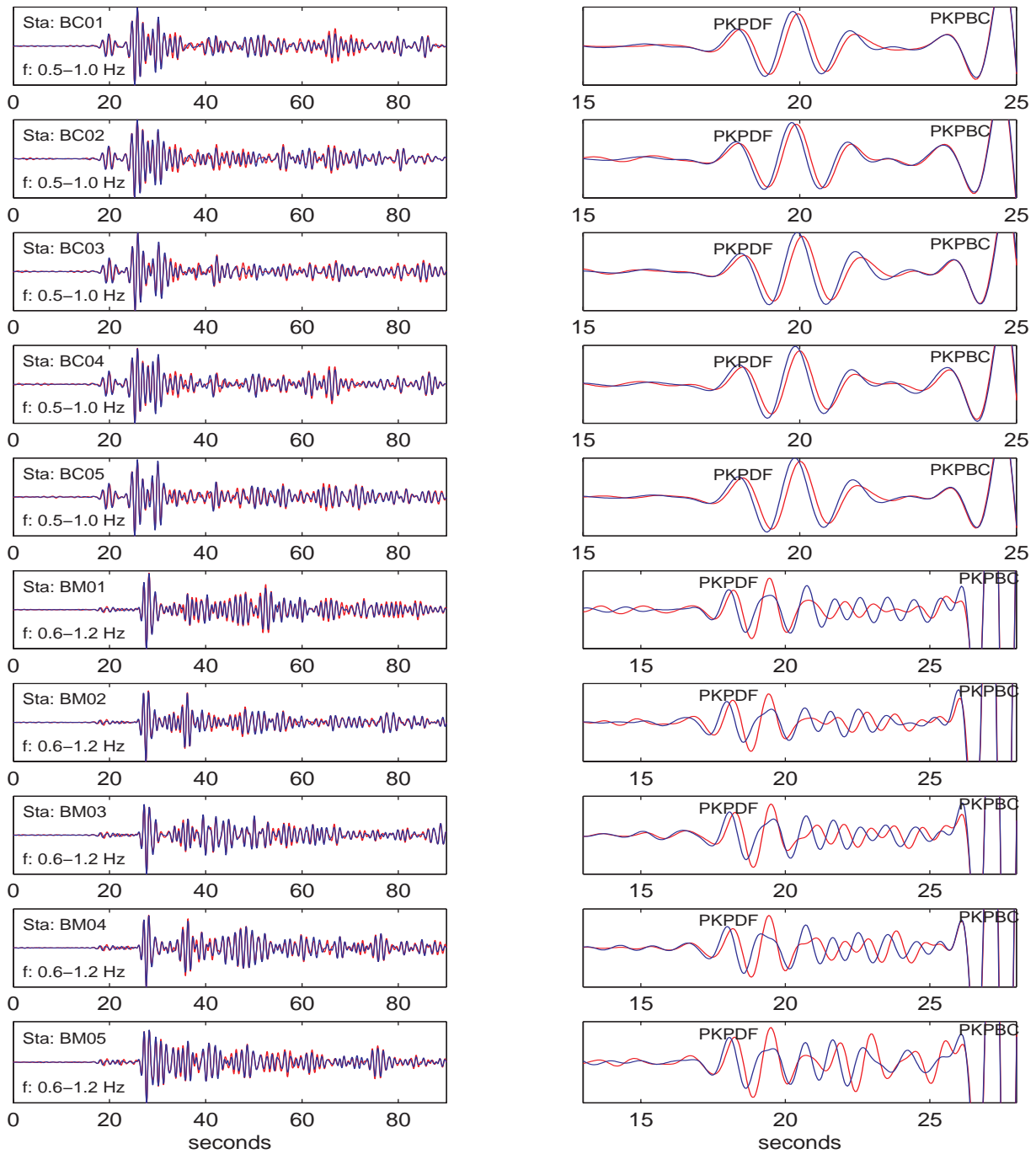
Fig. S4. (A) Waveform comparison of the doublet events 1993/12/01 (red) and 2003/09/06 (blue) at Beaver Creek array (BC01-BC05) and Burnt Mountain array (BM01-BM05). In each row, the left panel shows the overall waveform similarity and the right panel shows the delayed *PKP(DF)* arrival of the earlier event. The station code is marked in each panel on the left, as well as the pass-band of the waveforms, which is chosen for a good signal-to-noise level. The time window of the right panels could have different scales.
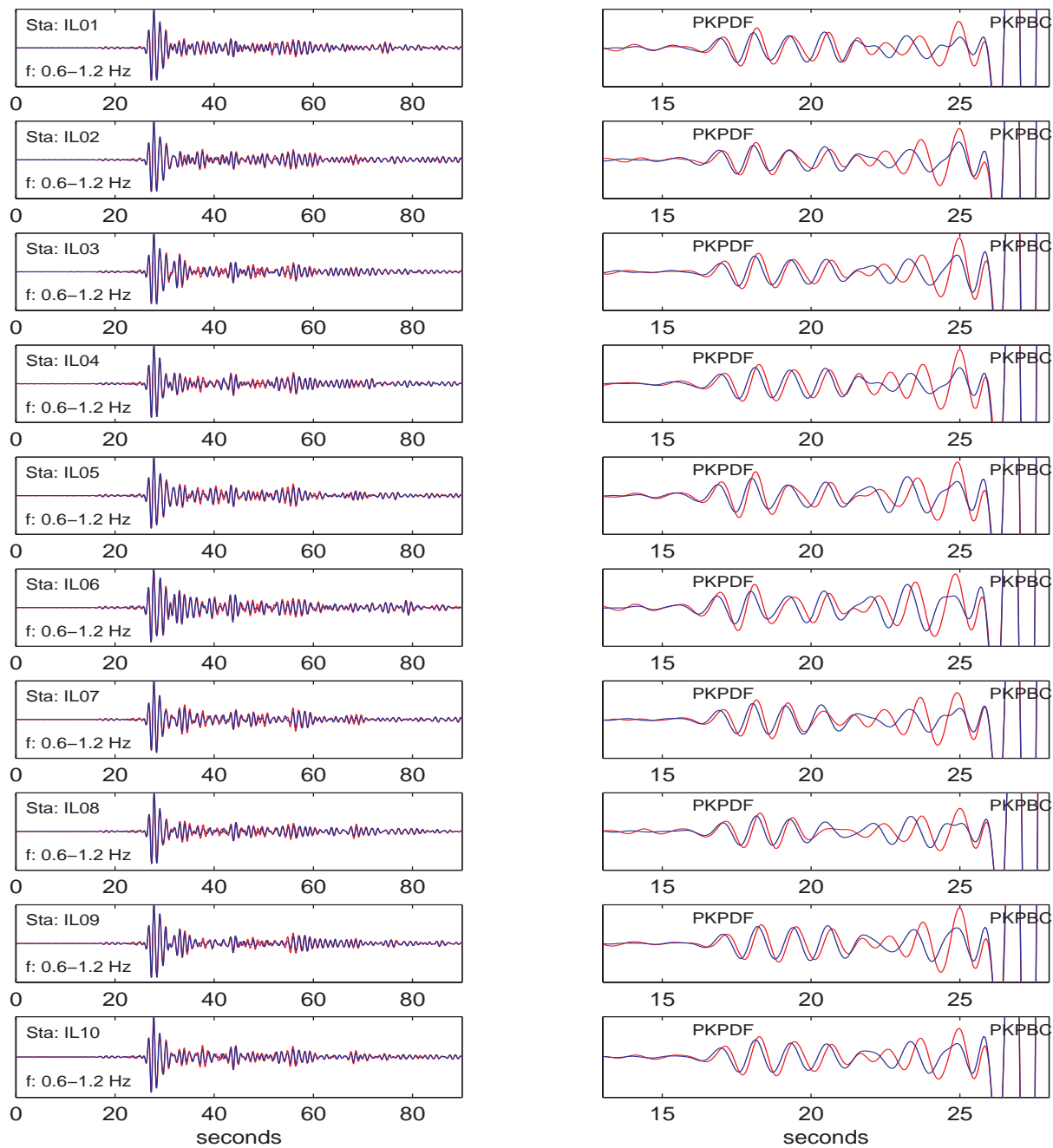
Fig. S4 (continued). (B) Same as **(A)** except for 10 channels at Eielson array (IL01-IL10).
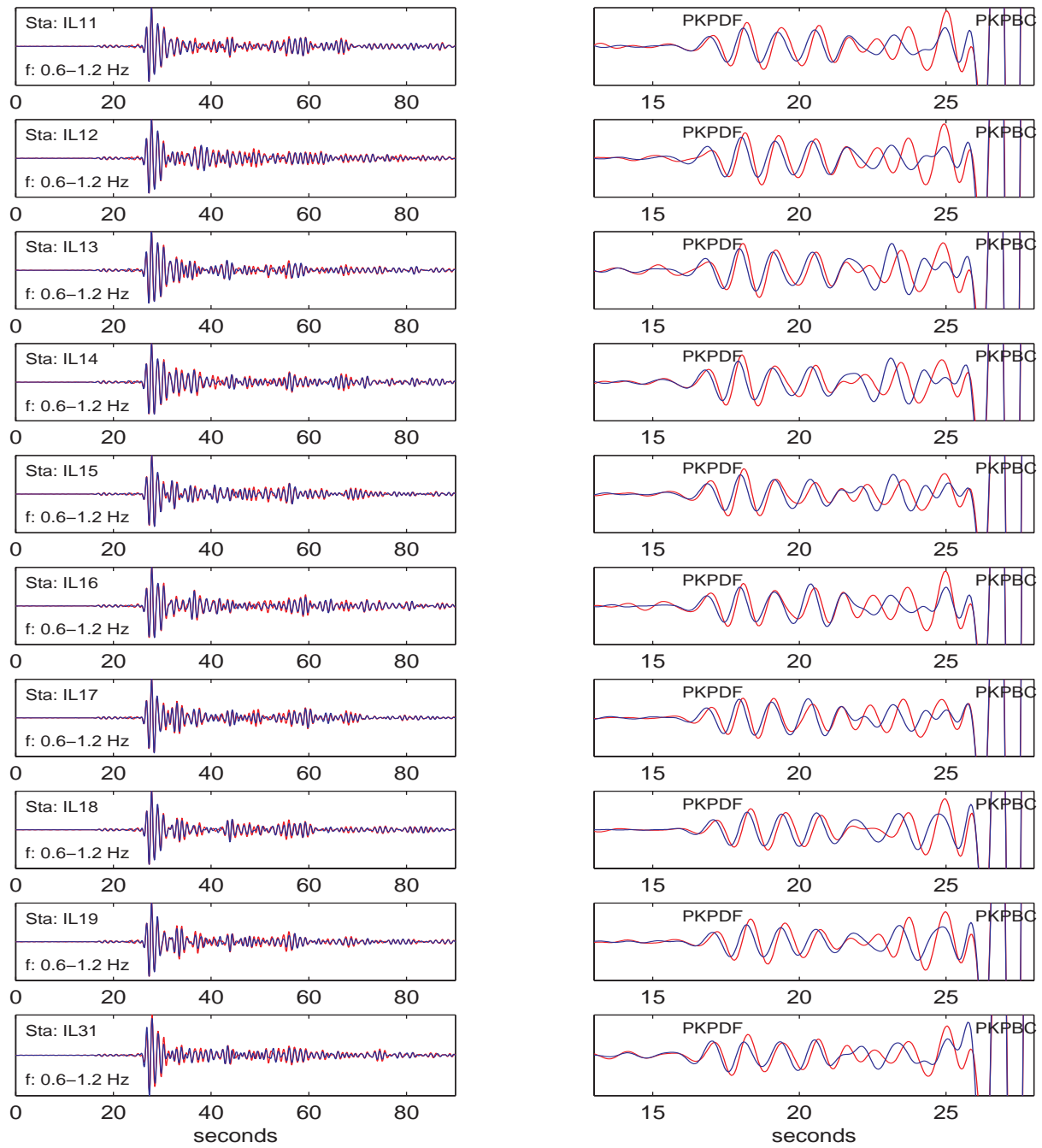
Fig. S4 (continued). (C) Same as **(A)** except for 10 channels at Eielson array (IL11-IL19, and IL31).
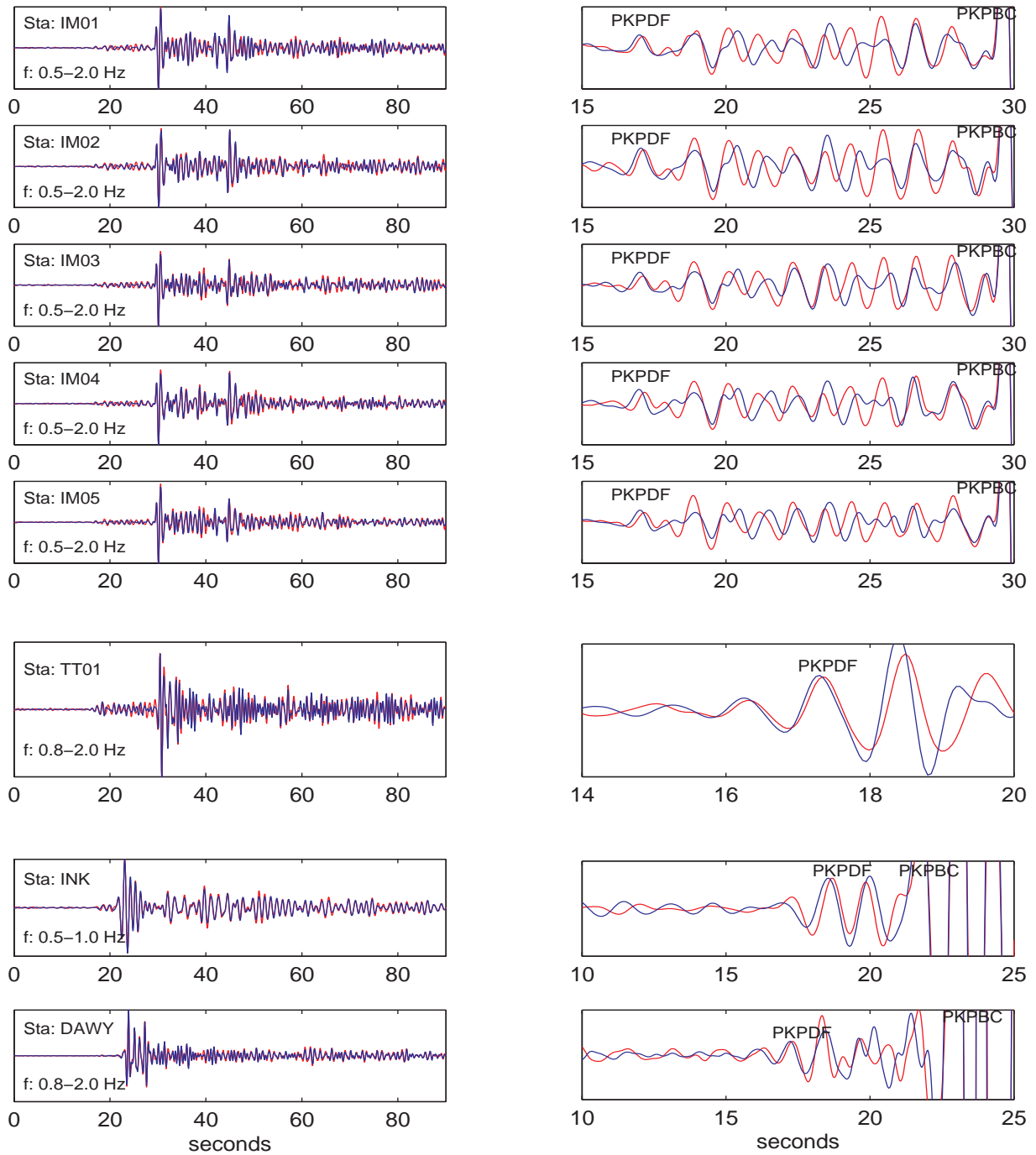
Fig. S4 (continued). (D) Same as **(A)** except for 5 channels at Indian Mountain array (IM01-IM05), station TT01, and two canadian stations INK and DAWY. Note that for the station TT01, the view of *PKP(DF)* part is enlarged and shown in a much shorter time window in order to observe a small but still positive *d(BC-DF)*.
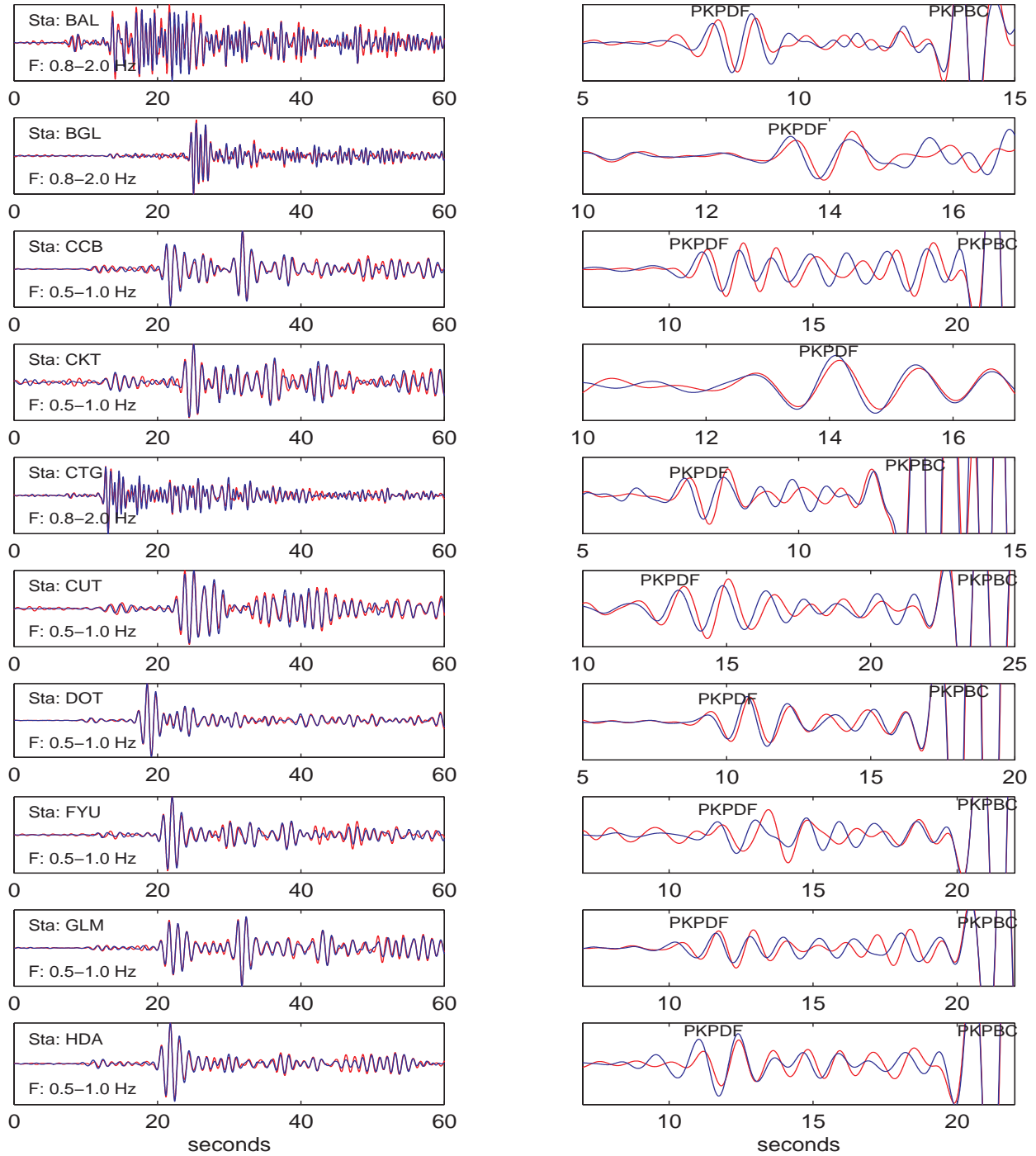
Fig. S4 (continued). (E) Same as **(A)** except for ASN stations: BAL, BGL, CCB, CKT, CTG, CUT, DOT, FYU, GLM, and HDA. Note that for the stations BGL and CKT, the view of *PKP(DF)* part is enlarged and shown in a much shorter time window in order to observe a small but still positive *d(BC-DF)*.
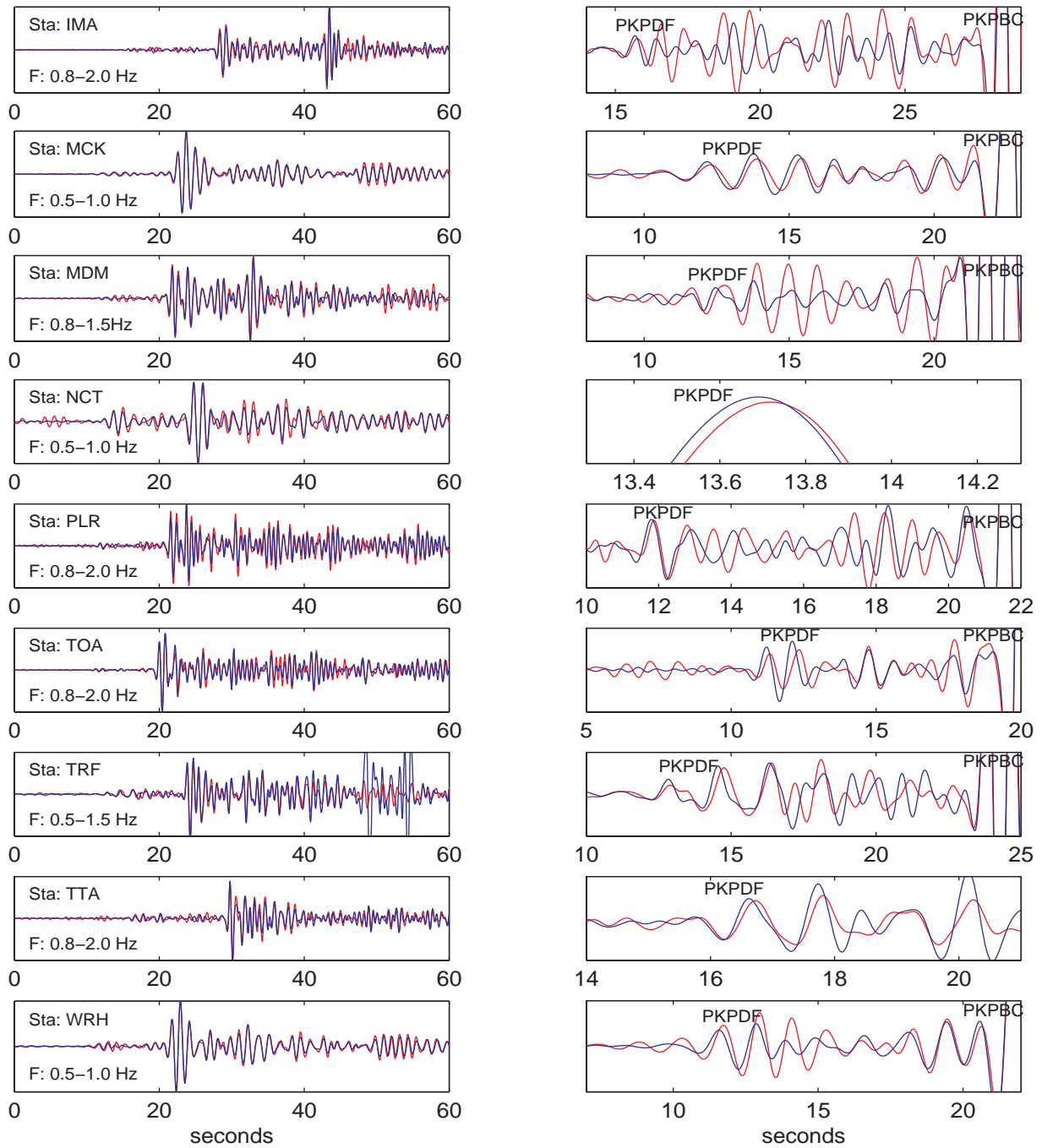
Fig. S4 (continued). (F) Same as **(A)** except for ASN stations: IMA, MCK, MDM, NCT, PLR, TOA, TRF, TTA, and WRH. Note that for the stations NCT and TTA, the view of *PKP(DF)* part is enlarged and shown in a much shorter time window in order to observe a small but still positive *d(BC-DF)*.
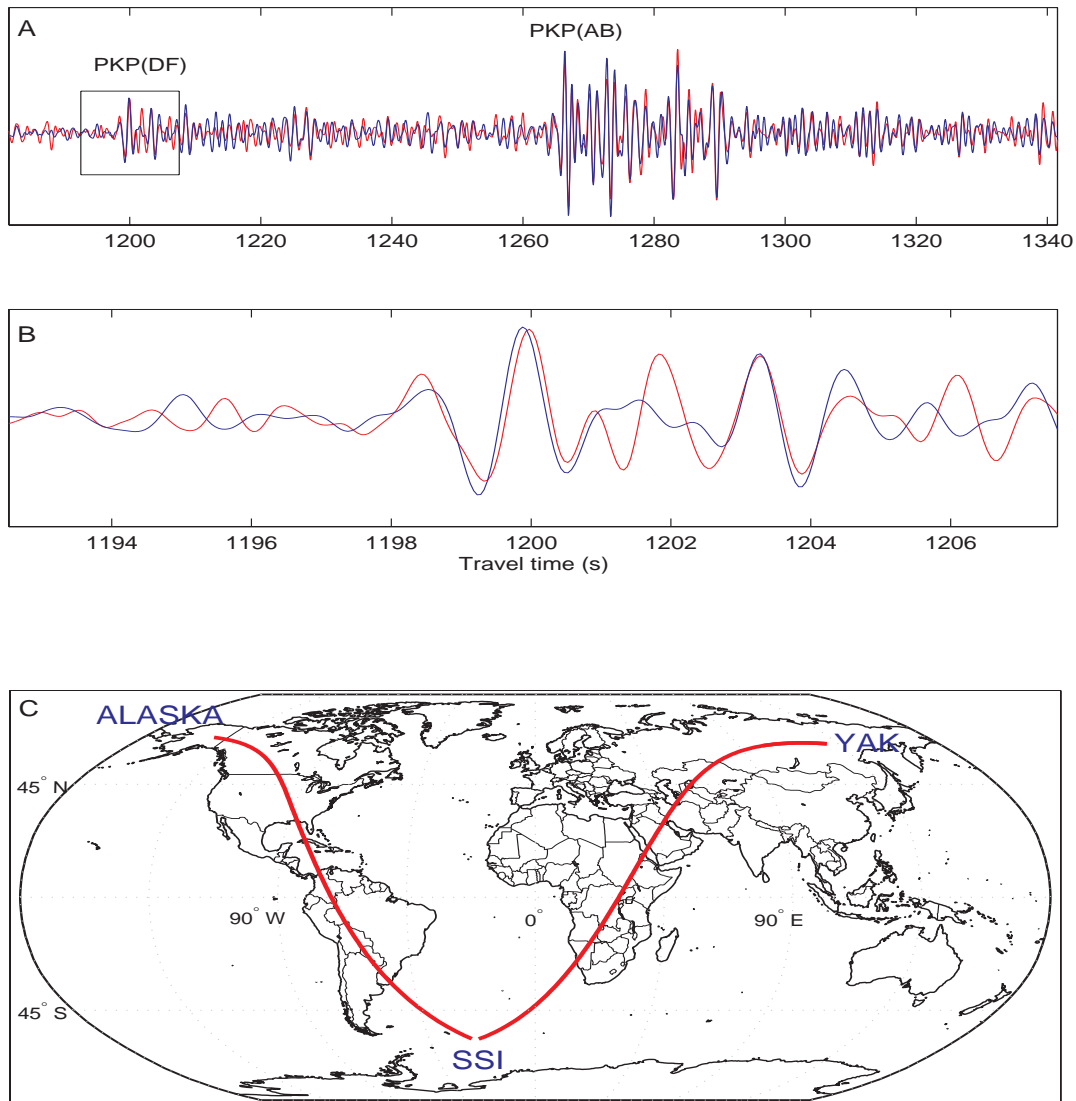
Fig. S5. Waveforms of the doublet events 1993/12/01 (red) and 2003/09/06 (blue) recorded at Yakutsk, Siberia (YAK) with a distance of about 167° from the SSI region. **(A)** Similar waveforms in the time window including the *PKP(AB)* phase. **(B)** Enlarged view of *PKP(DF)* waveforms from the box in (**A**). The observation shows a small temporal change of differential travel times between *PKP(AB)* and *PKP(DF)* phases, and some change in *PKP(DF)* coda. The waveforms are filtered from 0.5 to 1.1 Hz. **(C)** World map showing the ray path from SSI to Alaska and that from SSI to YAK. Such a path that samples a different depth and region of the inner core may be used to explore the inner core inhomogeneities and differential motion on a much larger scale than the local sampling of SSI-Alaska path as we presented in this study.
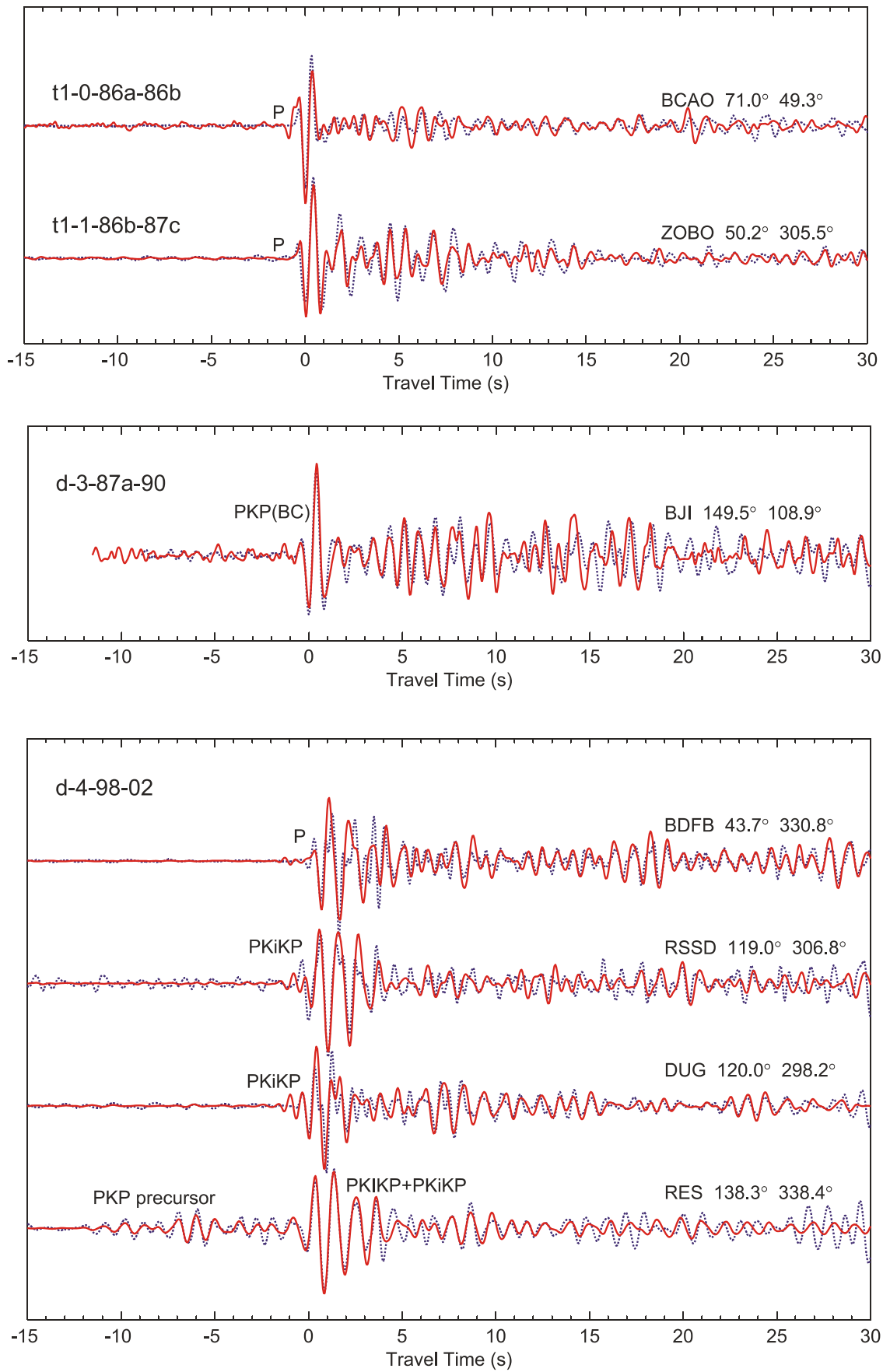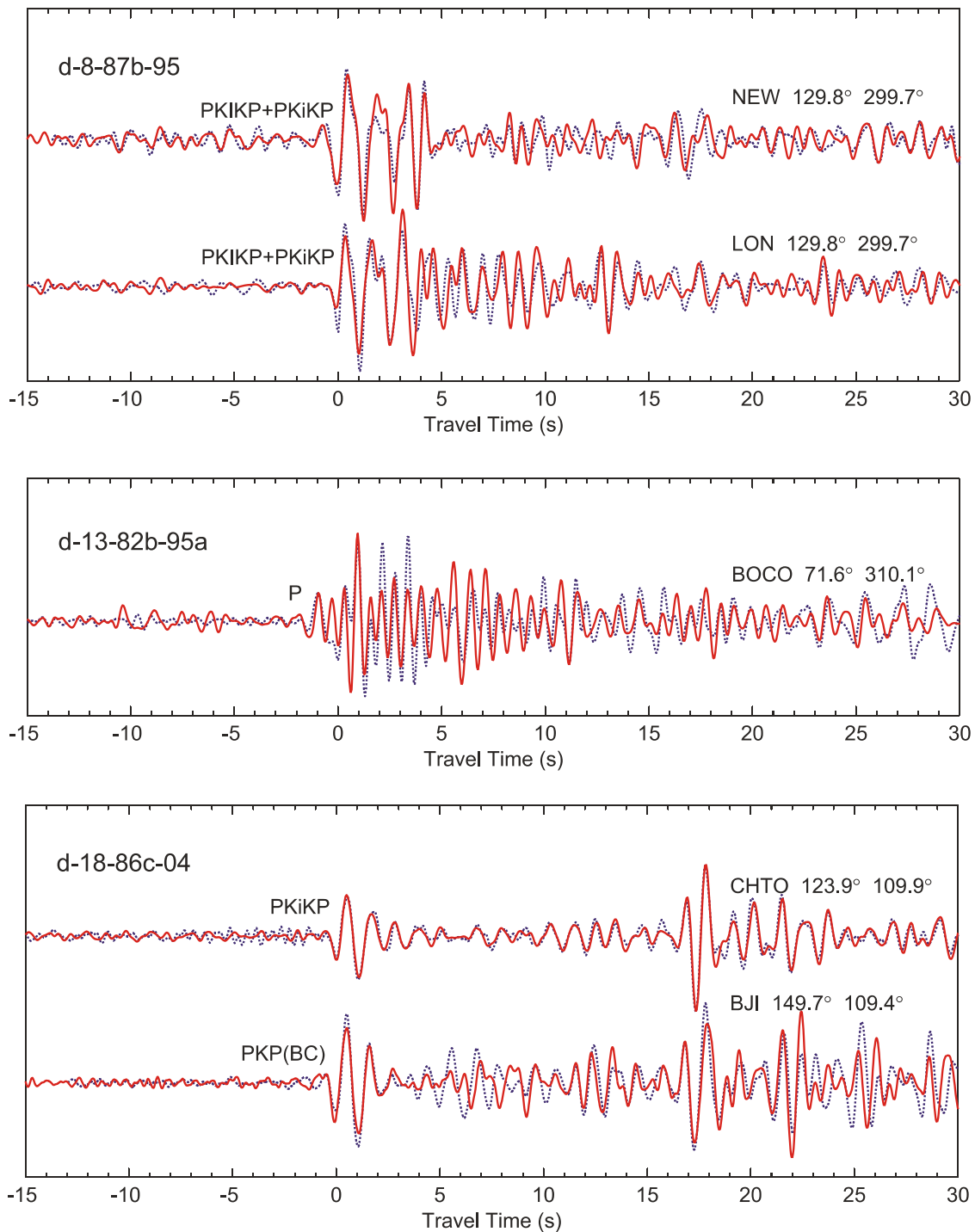
Fig. S6. P and PKP waveforms (vertical components) of SSI doublets recorded at stations besides COL station and Beaver Creek array. The early and later events of each doublet are indicated by the blue dashed and red solid traces, respectively. The epicentral distance and azimuth to each station are labeled next to the station name. Note, in particular, the similarity of the PKP precursor waveforms recorded at RES station in Canada for the 1998 and 2002 doublets (d-4-98-02).
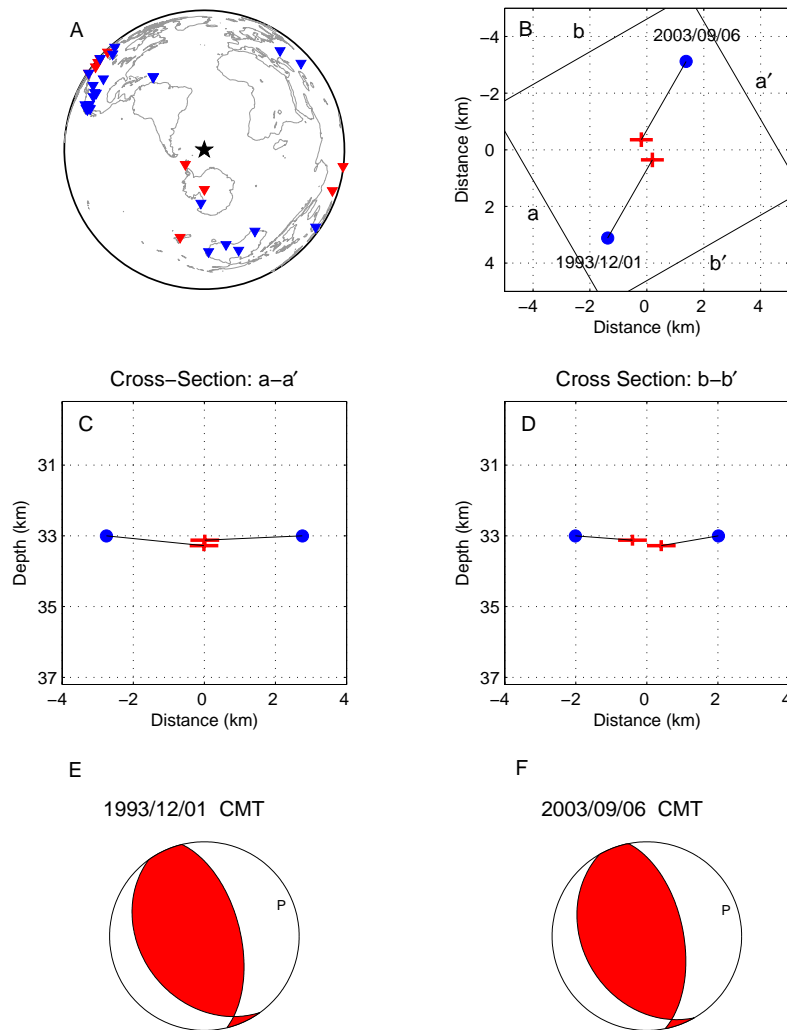
Fig. S7. Double-difference analysis of the relative location of the doublet 93&03. Least-squares errors are a few hundred meters horizontally, and less than a hundred meters vertically. (**A**) Map view of station locations showing the distance and azimuth coverage. Red triangles are stations with waveform cross-correlation measurements; blue triangles are stations with phase-pick measurements. (**B**) Map view of the relative relocation result. Red crosses are location and least-squares error estimates for the double-difference locations; blue dots are initial locations from Earthquake Data Report (EDR). (**C**) Cross-section view of relocation result along a-a'. (**D**) Cross-section view of relocation result along b-b'. (**E**) and (**F**) Harvard CMT solutions of the two events.
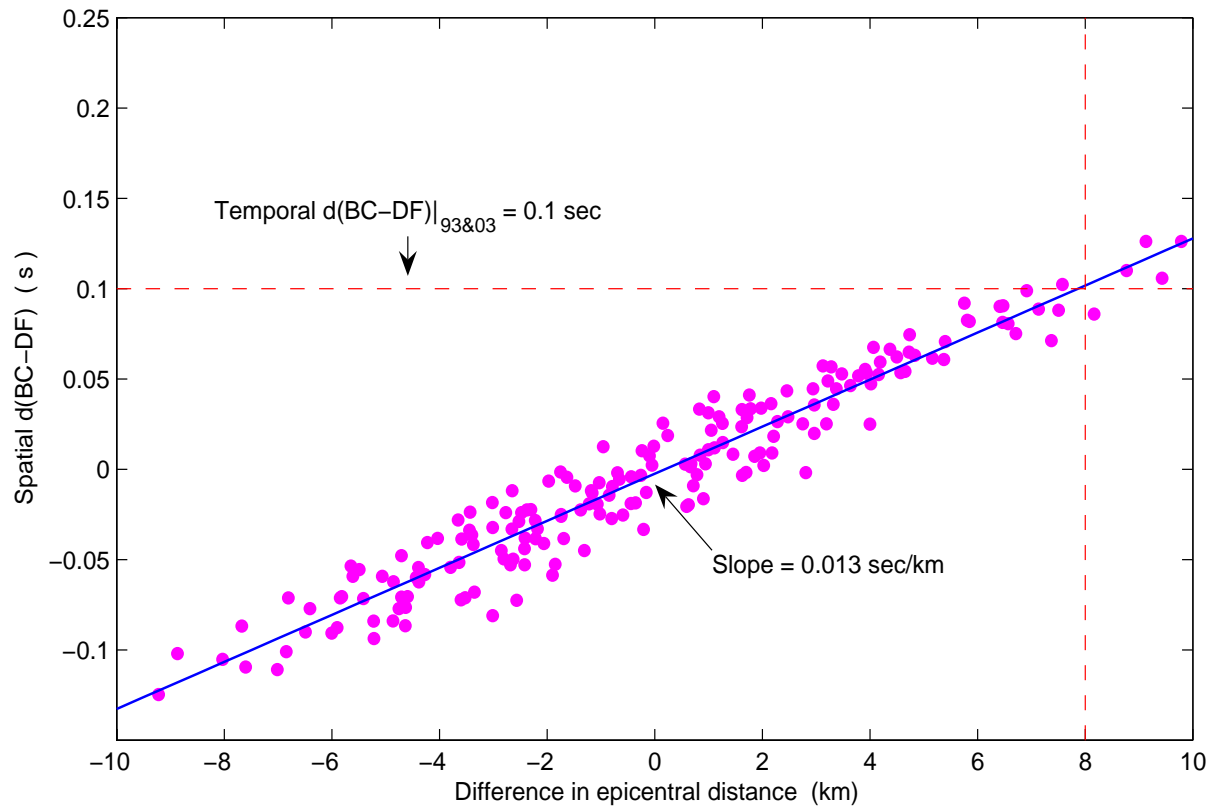
Fig. S8. Observed spatial change of differential travel times between *PKP(BC)* and *PKP(DF)* phases, abbreviated as *spatial d(BC-DF)*, for records of the earlier event 1993/12/01 of the doublet 93&03 at 20 channels of Eielson array in Alaska. The data is plotted as a function of difference in the epicentral distance between any two stations. The horizontal red dashed line represents the mean value of temporal change *d(BC-DF)* for the doublet 93&03, which is measured as 0.1 s at Eielson array with epicentral distance about 151° from the source; the vertical red dashed line indicates that at least a 8 km difference in epicentral distance for the two events is needed to cause the observed 0.1 s differential time, while our analysis shows that the two events are separated less than 1 km.
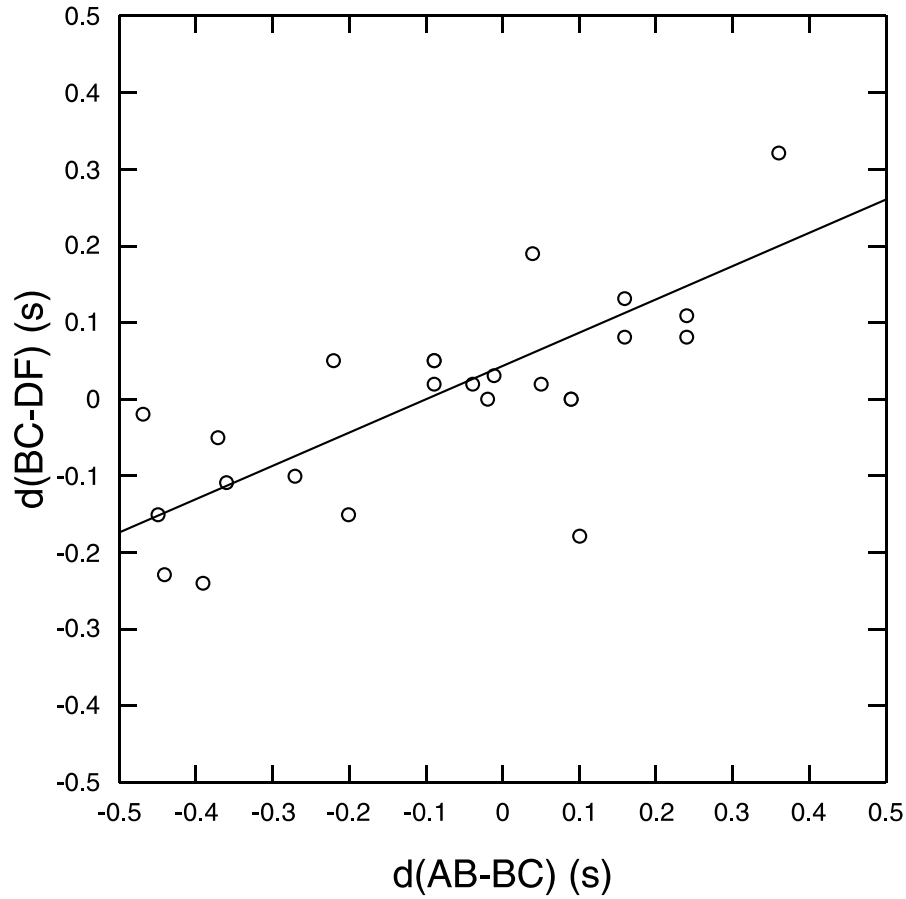
Fig. S9. Difference in BC-DF times vs difference in AB-BC times measured from earthquake pairs at somewhat different locations with time separation less than 5 years and similar waveforms. The data are from Song (2000b) and this study. The line is the linear regression without the outlier. The slope is 0.434 +/- 0.067 (one standard deviation). The slope is slightly smaller with the outlier (0.398+/-0.080). The regression can be used to calibrate d(BC-DF) when d(AB-BC) is slightly different from zero, to improve further the precision in estimating the rate of the BC-DF temporal change.
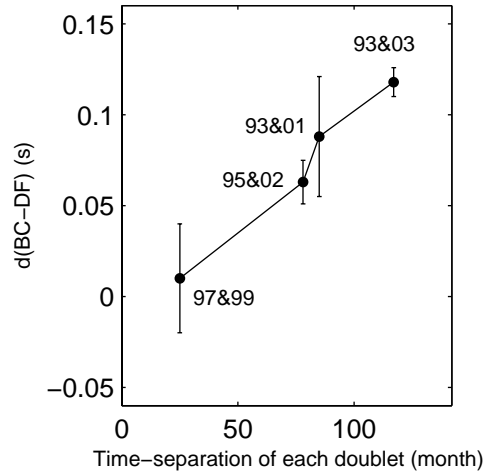
Fig. S10. Observed *d(BC-DF)* of four independent doublets at Beaver Creek array versus time-separation of the two events for each doublet. Dots are mean values of the measurements in the pass-band from 0.9 to 2.0 Hz at array channels for each doublet, the error bar is the standard deviation of the measurements.
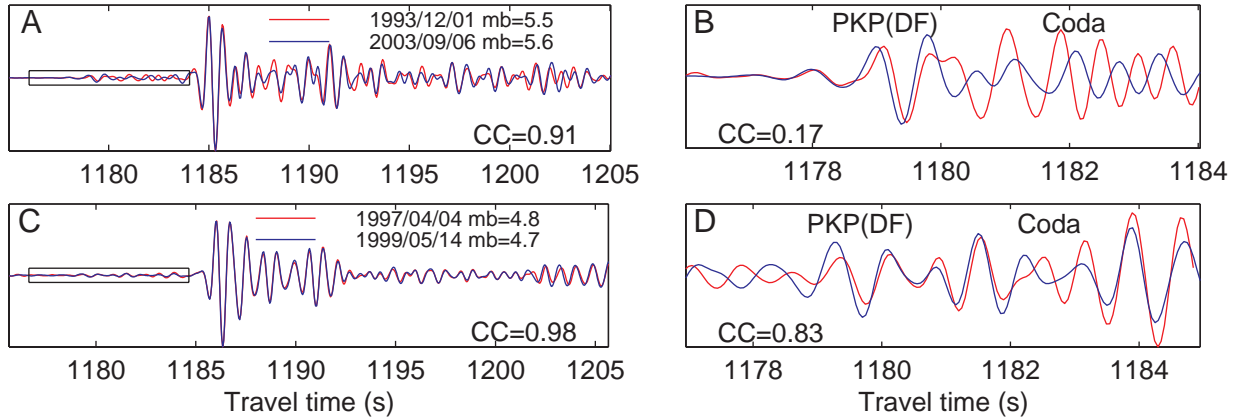
Fig. S11. *PKP(DF)* coda of two waveform doublets. (**A**) Aligned and overlapped waveforms of the doublet 93&03 recorded at the channel BC04 of Beaver Creek array in Alaska. (**B**) Enlarged *PKP(DF)* and its coda from the box in (**A**). (**C**) Aligned and overlapped waveforms of the doublet 97&99 recorded at the same channel as in (**A**). (**D**) Enlarged *PKP(DF)* and its coda from the box in (**C**). The waveforms are filtered from 1.0 to 2.0 Hz, and CC = cross-correlation.